LIGHTCURVE ANALYSIS FOR TEN NEAR-EARTH ASTEROIDS

Peter Birtwhistle
Great Shefford Observatory
Phlox Cottage, Wantage Road
Great Shefford, Berkshire, RG17 7DA
United Kingdom
peter@birtwhistle.org.uk

(Received: 2021 Jan 3)

Lightcurves and amplitudes for ten near-Earth asteroids observed from Great Shefford Observatory during close approaches in 2018 and 2020 are reported: 2018 KF1, 2020 GF2, 2020 OH3, 2020 RA6, 2020 RZ6, 2020 TP1, 2020 TD8, 2020 UQ6, 2020 VZ6 and 2020 XX3. 2020 UQ6 is the largest, with H = 22.6, all others are small objects, H > 24.5. Seven have superfast rotation periods, P < 10 min, including 2020 RZ6 and 2020 TD8 with P < 1 min.

Photometric observations of near-Earth asteroids during close approaches to Earth in 2018 and 2020 were made at Great Shefford Observatory using a 0.40-m Schmidt-Cassegrain and Apogee Alta U47+ CCD camera. All observations were made unfiltered and with the telescope operating with a focal reducer at *f*/6. The 1K×1K, 13-micron CCD was binned 2×2 resulting in an image scale of 2.16 arcsec/pixel. All the images were calibrated with dark and flat frames. *Astrometrica* (Raab, 2018) was used to measure photometry using APASS Johnson V band data from the UCAC4 catalogue. *MPO Canopus* (Warner, 2020), incorporating the Fourier algorithm developed by Harris (Harris et al., 1989), was used for lightcurve analysis.

2018 KF1. An Amor object with estimated diameter of 21 m and a perihelion distance of 1.01 AU was discovered by the Catalina Sky Survey on 2018 May 19 (Bacci et al., 2018) and had a close approach of 2 Lunar Distances (LD) on 2018 May 21.36 UT. A search of the Astrophysics Data System (ADS, 2020), the Asteroid Lightcurve Database (LCDB, Warner et al., 2009), and wider searches did not find any previously reported results for 2018 KF1. It was observed for 3.25 hours on the night of 2018 May 20/21, moving at ~110 arcsec/min.

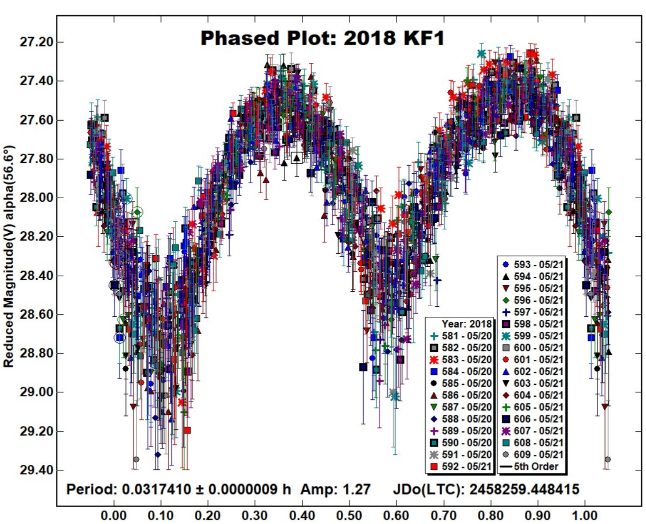

Large variations in brightness were evident between consecutive short exposures taken early in the evening for astrometry and so for photometry, exposures were kept to less than 4 seconds to keep the object from trailing and to ensure potential lightcurve smearing was reduced (Pravec et al., 2000). The asteroid reached apparent magnitude +16 and was visible in all images, but only weakly recorded at some of the deepest minima. Using 1,498 data points, an asymmetrical bimodal lightcurve is evident with a superfast rotation period of 1.9 minutes. 2018 KF1 completed 102 rotations during the 3h 45 m it was under observation.

2020 GF2. This Apollo object was well observed by a number of observatories in the three days following the discovery by the ATLAS team on 2020 Apr 10 (Melnikov et al., 2020a).

No previously reported results have been found in the ADS, LCDB, or from wider searches. 2020 GF2 passed Earth by 2.4 LD on 2020 Apr 12.5 UT and was a mag 16-17 object throughout. It was followed at Great Shefford on the night of 2020 Apr 11/12 and 1,417 images were measured from exposures ranging from 2 - 4.6 seconds. The sky motion reached 122 arcsec/min and the short exposures kept the trailing within the 3-pixel radius measurement annulus used in *Astrometrica*.

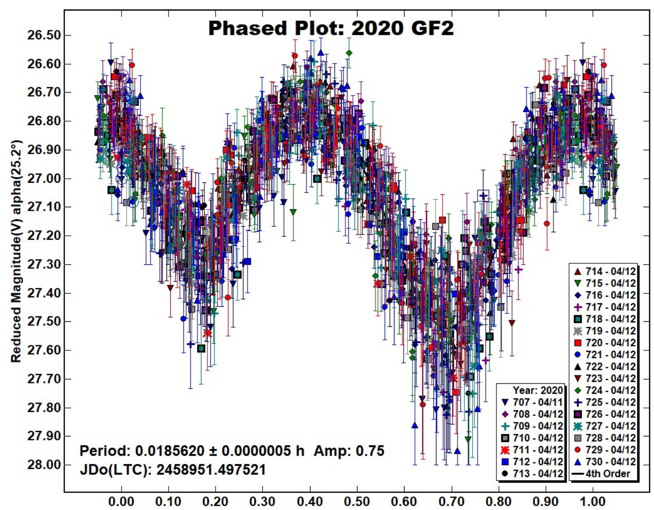

2020 GF2 is another small (estimated 19 m diameter) superfast rotator with a period of 1.1 minutes. 174 rotations occurred during the 3h 14 m it was under observation.

2020 OH3. An ATLAS discovery from Mauna Loa on 2020 July 22.56 UT (Melnikov et al., 2020b) with an estimated diameter of 36 m was a 16th magnitude target of opportunity on the night of 2020 July 22/23 from Great Shefford. It was under observation for 2.5 hours, moving at ~100 arcsec/min at a range of 5.4 LD and would pass Earth at 5.1 LD on 2020 July 23.46 UT, but moving swiftly south, would be below the horizon by the next night.

Exposures were limited to 4 seconds to allow the asteroid trail to be enclosed within the measurement annulus in *Astrometrica* and the apparent speed dictated that the telescope needed to be repositioned 12 times. 1,076 images were used in the analysis, indicating an only slightly asymmetric bimodal lightcurve with P = 23.5 min. There are no previous entries for 2020 OH3 in ADS or the LCDB.

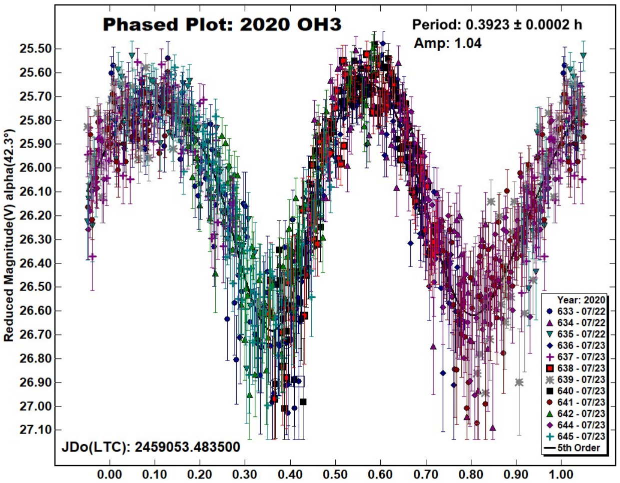

2020 RA6. An Apollo object with estimated diameter 19 m was discovered by the ZTF team at Palomar on 2020 Sep 14 with pre-discovery astrometry reported by Pan-STARRS 1 & 2 and Mt. Lemmon back to 2020 Sep 6 (Buzzi et al., 2020). It made an approach to within 1.4 LD of Earth on 2020 Sep 18.04 UT; it was observed from Great Shefford from 2020 Sep 17.84 UT for 27 minutes and then 3 hours later for a further 22 minutes (Table I).

No previous results for 2020 RA6 were found in the ADS, in the LCDB, or from wider searches. Apparent speed increased from 310 to 410 arcsec/min during the period and exposures were limited to 1 second throughout so that trailing of the target would always be enclosed within a 13 arcsec diameter measurement annulus used in *Astrometrica*. It is noted that 2020 RA6 passed 67 arcmin from the N. Celestial Pole on 2020 Sep 17.986 UT, which increased the length of time required to reposition the telescope. Peak-to-peak variations in magnitude were evident every ~10 minutes and at minimum brightness the individual measurements had low SNR. Three sets of images taken at minimum light were stacked in *Astrometrica* to increase signal strength, with 11-12 individual exposures being selected for each stack, resulting in each stack spanning a maximum of 44 seconds of time. These allowed four higher SNR measurements to be made for each of these three sets of images. Because the length of the two observing runs were similar to the apparent rotation period, the period spectrum shows multiple potential solutions.

Bimodal curves occur at ~0.33 h, with trimodal solutions appearing around 0.5 h and quadrimodal above 0.55 h.

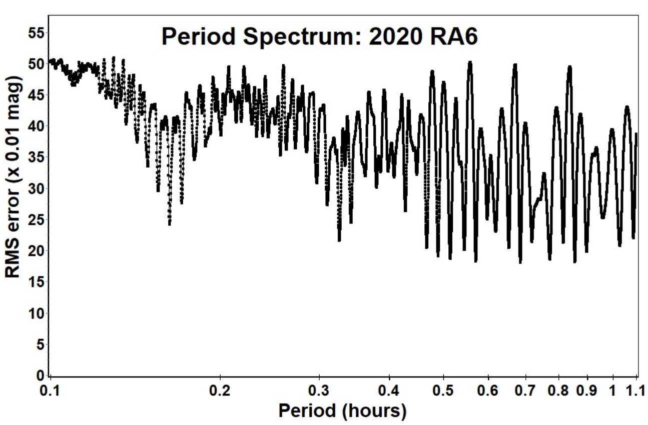

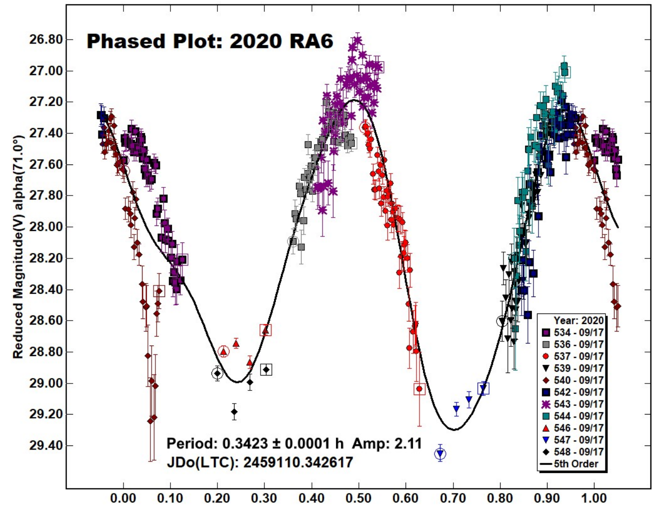

With the short coverage unable to discount longer periods, a bimodal solution is assumed here. The two strongest bimodal solutions were investigated (0.3265 h and 0.3423 h), representing a difference of 0.5 of the period over the observed arc. The longer period is preferred since, although the RMS was slightly greater, the direction of slope of the derived curve fitted the observations better.

The phase angle increased by 20° to $\alpha > 90°$ during the time under observation and the amplitude is likely to have increased and caused some extra scatter in the solution. It is noted that an anomalous fade of ~1 magnitude is apparent in a single set of measures centred at phase 0.06, from images spanning ~60-90 seconds.

2020 RZ6. The ATLAS system on Haleakala discovered this small Apollo (estimated diameter 14 m) on 2020 Sep 15 (Tichy et al., 2020), two days before passing just inside the orbit of the Moon, reaching 0.9 LD on 2020 Sep 17.77 UT. No previous results were found in the LCDB or from wider searches. Three separate sets of images were obtained in the hours after closest approach (Table I). Exposures were initially limited to 1 second due to the fast 315 arcsec/min apparent speed, but were increased to 1.5 seconds by the last run as the speed reduced to 195 arcsec/min.

Large variations in brightness were immediately evident between consecutive exposures and some of the deepest minima were either below the limiting magnitude or too faint to be measured reliably; however, the majority of the exposures were usable. As a fast rotation period was suspected, a period spectrum was produced in *MPO Canopus* searching for short periods in the range 18 seconds up to 6.3 minutes.

This initial search indicated that a quadrimodal solution with period 0.01771 h was preferred. However, the step size in this coarse period spectrum was 1×10^{-5} h and examining the bimodal and quadrimodal times with a finer step size of 1×10^{-7} h showed that the initial search was too coarse and the bimodal solution was actually a significantly better fit. The period spectrum figure shows the rejected solutions marked with crosses and the accepted bimodal solution with a tick.

There was a 3.9 h gap between runs 1 and 2 and then a further gap of 2.1 h between runs 2 and 3. Independent reductions from the three runs all produced similar periods and lightcurves. However, trying to fit all three runs together was not satisfactory, introducing significantly more noise to the lightcurve. During the time 2020 RZ6 was under observation it was receding from Earth and the phase angle was also increasing by 2.4°/h from 86° to 103°. The ephemeris, calculated with G = 0.15 in the H-G system predicted the brightness would be fading by 0.17 mag/h but at the high phase angles encountered, this can only be taken as a very rough guide. The photometry indicated a much slower fall of ~0.085 mag/h. *MPO Canopus* was used to vary the adopted value of G to find a minimum in the RMS of the fitted curve. The RMS was reduced from 0.32 to a minimum of 0.23 using a value of G = -0.25 and this value has been used to produce the lightcurve, including all 550 data points. Derived at such high phase angles, this value of G does not represent the lightcurve well at smaller phase angles, e.g., the discovery astrometry at phase angle 53° lists magnitudes that are ~1.4 mag fainter than this value of G would predict.

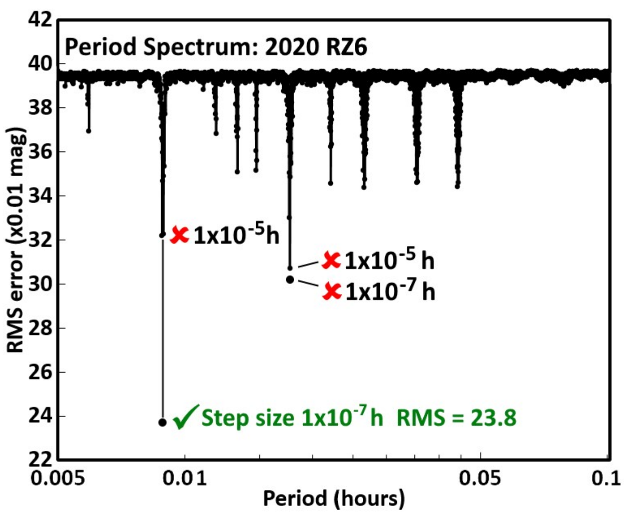

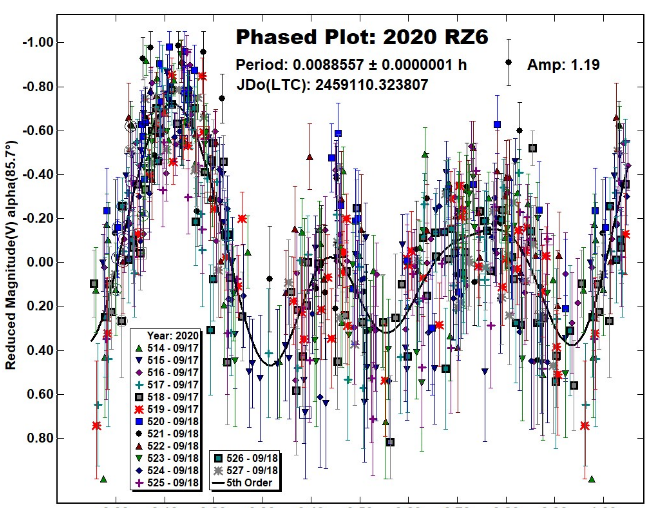

2020 RZ6 is a superfast rotator with a period of 31.9 seconds and completed 46 revolutions in run 1, 22 in run 2 and 35 in run 3. Independent of the lightcurve solution in *MPO Canopus*, a check was made to see whether the three runs could be unambiguously linked by estimating the likely error in the number of rotations ΔN when propagating a calculated period with its associated error to another time, derived from Eq (3) in Kwiatkowski et al. (2010) by:

$$\Delta N \approx \Delta t \, \Delta P / P^2. \quad (1)$$

where Δt is the time interval separating two individual lightcurves, P is the period from one of the individual solutions, and ΔP is the maximum period uncertainty, in practice taken here to be 3× the formal uncertainty from *MPO Canopus*, and Δt, ΔP and P in the same units. For a bimodal curve ΔN < 0.25 implies a maximum (or minimum) can be matched unambiguously, less than ¼ cycle from reality. The error propagated from run 3 to run 2 (a shorter interval than run 1 to 2) is ΔN = 0.21, allowing runs 2 and 3 to be linked unambiguously. The revised period and error from a solution combining runs 2 and 3 then allowed linking run 2 to run 1 with ΔN = 0.04. The lightcurve using all three runs indicates that 2020 RZ6 completed a total of 775 revolutions during the observing period. Since the minima of the lightcurve were incompletely covered, it is likely that the actual amplitude is somewhat larger than the calculated value of 1.19 mag.

2020 TP1. This ~13 m diameter Apollo was discovered by the ATLAS-HKO, Haleakala team on 2020 Oct 9 at a distance of 3 LD, already receding from Earth after passing just inside 1 LD 20 hours earlier (Pettarin et al., 2020). A search of the ADS, the LCDB, and wider searches did not find any previously reported results for 2020 TP1. It was observed for 93 minutes starting at 2020 Oct 9 19:34 UT and then again for 104 minutes starting the same night at 22:17 UT (Table I). No obvious superfast rotation had been evident during earlier image acquisition for astrometry and with sky motion at 26 arcsec/min, 16 second exposures were taken for photometry.

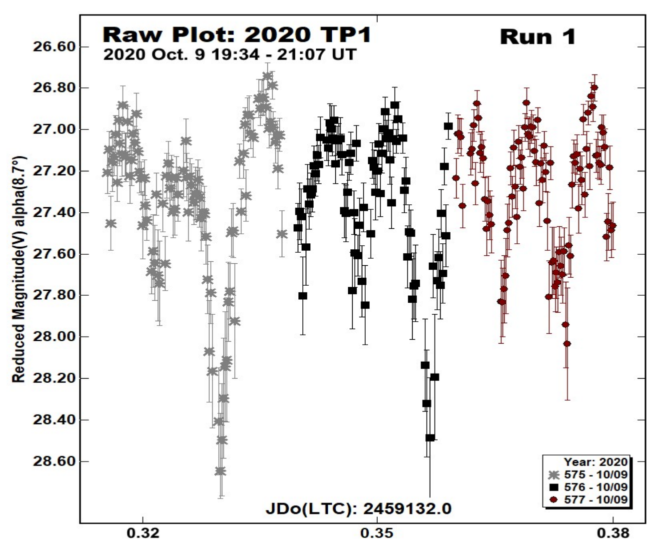

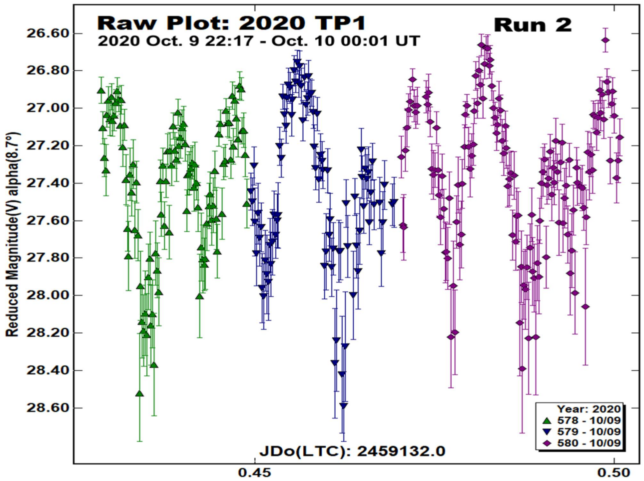

A period spectrum shows a bimodal solution at 0.42 h, but with the best fit being a trimodal one at 0.63 h and solutions at 0.83 h and 1.04 h, all having slightly better RMS fits than the bimodal one. The raw plots of the two periods of observation, run 1 and run 2, show regular variations of about 0.7 magnitudes amplitude every ~12 minutes, but with every third minima being very deep.

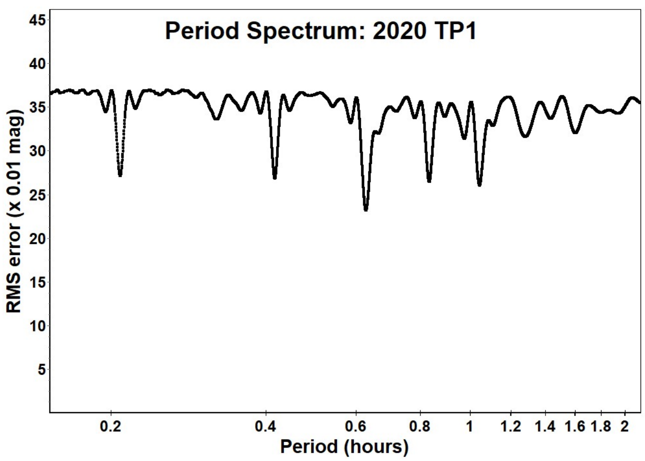

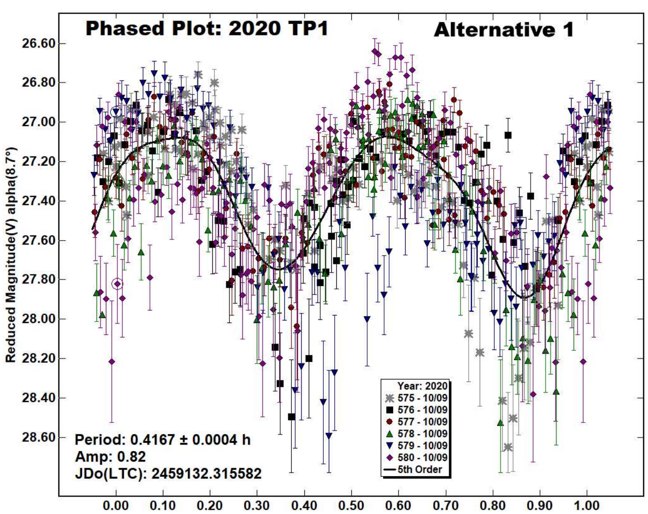

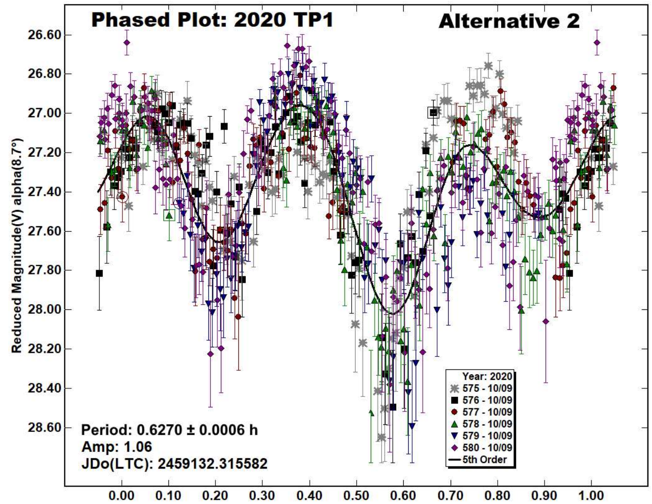

Additionally, the three maxima between these minima appear relatively equal during run 1 but are progressively unequal during run 2. Lightcurves are given for bimodal (alternative 1) and trimodal (alternative 2) solutions, but significant trends in both may indicate that 2020 TP1 is tumbling This is not resolved conclusively, so it is expected to be rated as PAR = -1 (Non-Principal Axis rotation possible, but not conclusively) on the scale of Pravec et. al. (2005).

2020 TD8. Pan-STARRS 2 discovered this small Apollo object 12 days before it made a close approach to 1.6 LD on 2020 Oct. 27.36 UT (Jahn et al., 2020). No previously reported results for 2020 TD8 were found in the ADS, the LCDB, or from wider searches. It was followed over a period of 3.7 h starting 11.5 hours before closest approach, when it reached apparent magnitude +16. With the fast apparent motion of ~125 arcsec/min, exposures were limited to 2 and 3 seconds to keep trailing short enough to allow measurement in a 3-pixel radius annulus in *Astrometrica*. Large variations in brightness were obvious between consecutive exposures and it was only recorded weakly in some of the images at minima and occasionally not visible at all but 582 images were able to be measured.

A period spectrum shows the bimodal solution at 0.008 h to be marginally the strongest and, with the level of noise present, none of the other periods can be justified.

2020 TD8 is another superfast rotator with a period of 29.6 seconds. It is noted that it is included in the JPL Sentry Impact Risk Data table (JPL, 2020b) as a 14 m diameter virtual impactor, with a series of low probability potential impacts listed from 2045 onwards.

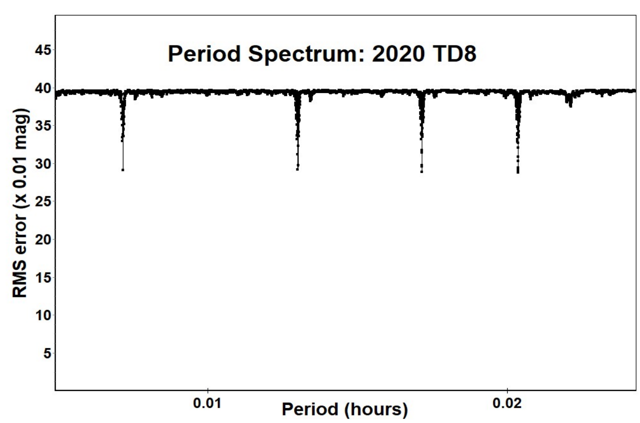

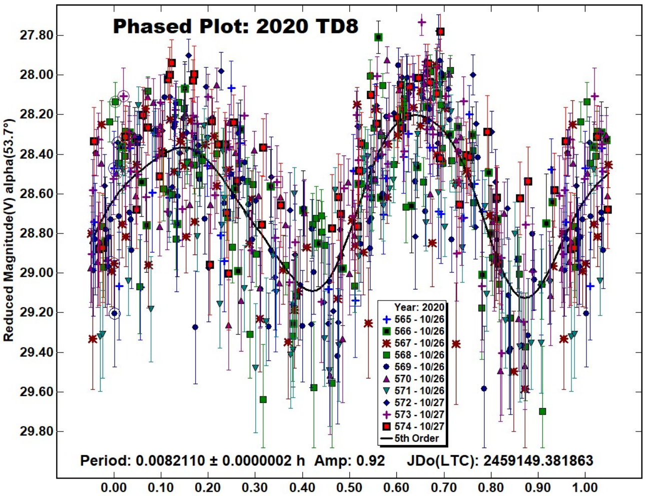

2020 UQ6. This Apollo with an estimated diameter of 90 m was discovered at magnitude 14 with the 1.05-m Schmidt at the Tokyo-Kiso station on 2020 Oct 27 and had passed Earth at 0.010 AU the day before. (Beniyama et al., 2020). When observed on 2020 Oct 28.0 UT it was 15th mag and 10 s exposures were taken over a period of 2 h 39 m resulting in 440 points being measured for the analysis.

A search of the ADS and the LCDB did not find any previously reported results for 2020 UQ6 but wider searches located a preliminary result published on Twitter (Wells and Bamberger, 2020) of $P = 0.04519 \pm 0.00005$ h, amp = 0.74 mag, agreeing well with this analysis.

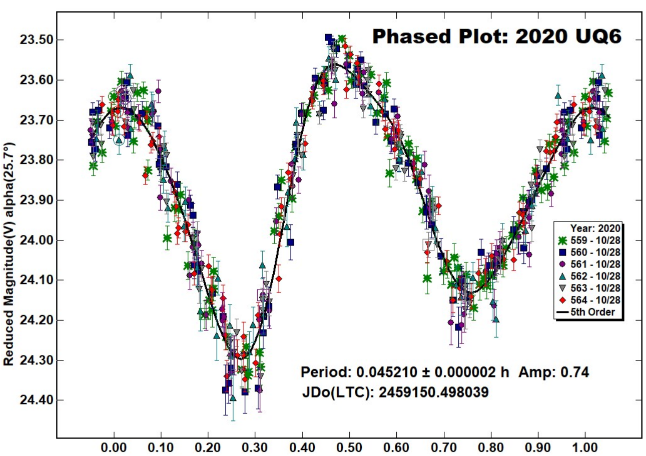

2020 VZ6. This Apollo with an estimated diameter of 27 m was submitted to the NEO Confirmation Page (MPC, 2020) as a magnitude 17 object by the ATLAS team on the night of the full Moon, 2020 Nov 30, but was subsequently matched with a magnitude 21 object observed from Mt. Lemmon and PanSTARRS two weeks earlier (Panterotto et al., 2020). It passed the Earth at 0.9 LD on 2020 Dec 3 and was followed from Great Shefford for 73 minutes on 2020 Dec 1. It was then at a distance of 3.5 LD, moving at 20 arcsec/min at low altitude, < +34°, in poor conditions with occasional high cloud interruptions and with the Moon 1 day past full, 48° distant. Exposures were 8 and 12 s and 333 points used to produce the rather noisy curve indicating a bimodal solution with a period of 5.9 minutes. No entries for 2020 VZ6 were found in the LCDB or in wider searches.

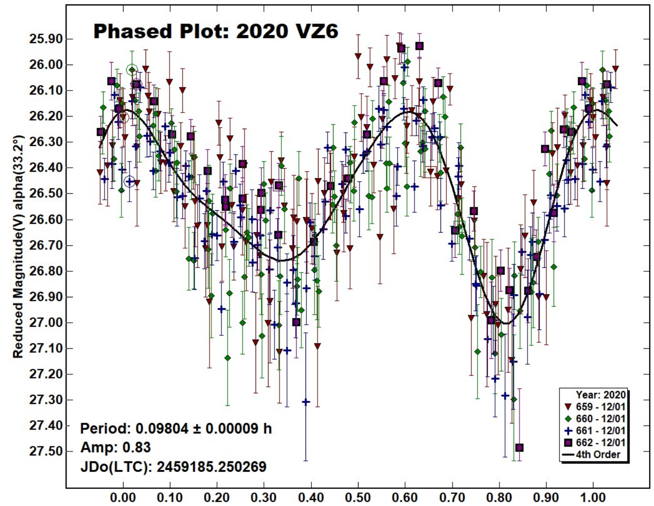

2020 XX3. A very small, 6 m diameter Apollo discovered by Pan-STARRS 1 (Read et al., 2020) 8 days before passing Earth on 2020 Dec 18.3 UT at 0.15 LD was followed over a 1 h 40 min period on 2020 Dec 17.0 UT when it was 16/17th mag and moving at 20 arcsec/min. Exposure length was set at 16 s but soon reduced to 10 s when it became obvious that a large drop in magnitude between consecutive exposures was occurring every ~2.3 minutes, in case finer resolution of the lightcurve would be useful. 17 of the longer exposures and 381 of the shorter were used in the lightcurve analysis. The period spectrum shows that a bimodal lightcurve of period 0.038 h (2.28 min) gives a slightly better fit than the quadrimodal solution at 0.076 h.

A split halves plot shows that the two halves of the quadrimodal solution are almost identical, so the bimodal solution is adopted.

No previously results have been found in the LCDB or from wider searches. It is noted that 2020 XX3 is included in the JPL Sentry Impact Risk Data table (JPL, 2020b) as a virtual impactor, with four very low probability potential impacts listed, starting in 2086.

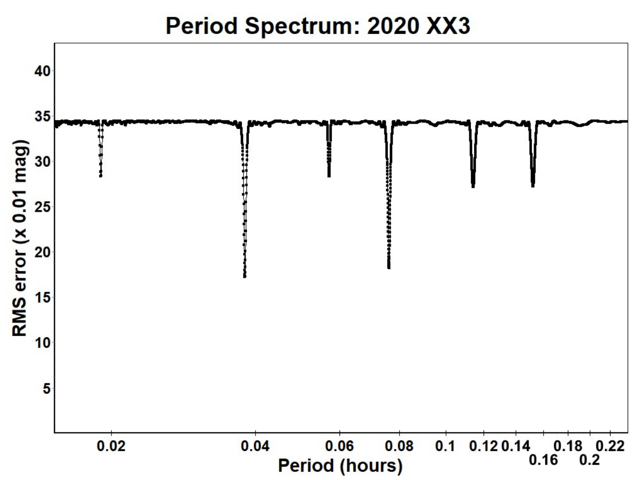

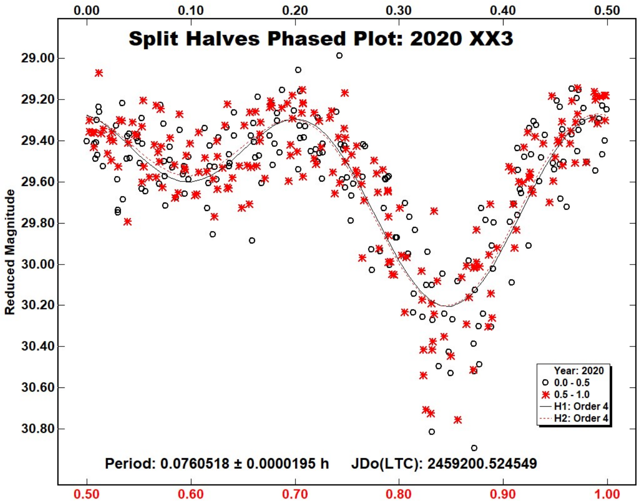

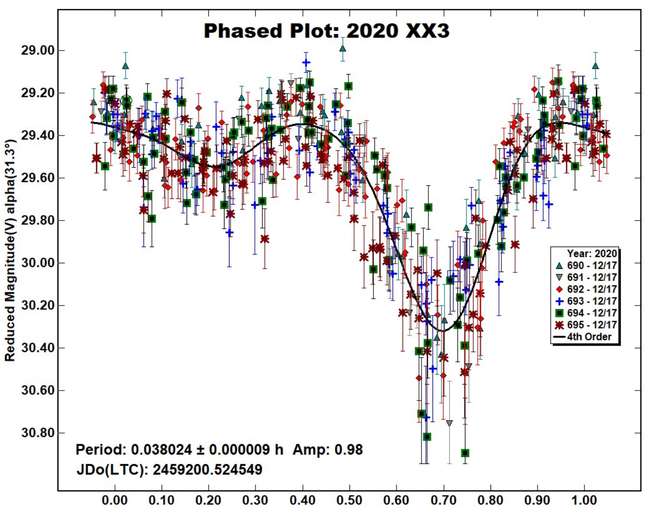

References

ADS (2020). Astrophysics Data System. *https://ui.adsabs.harvard.edu/*

Bacci, P.; Maestripieri, M.; Tesi, L.; Fagioli, G.; Jaeger, M.; Prosperi, E.; Vollmann, W.; Africano, B.M.; Christensen, E.J.; Fuls, D.C.; Gibbs, A.R.; Grauer, A.D.; Groeller, H.; Johnson, J.A.; Kowalski, R.A. and 22 colleagues (2018). "2018 KF1" *MPEC* 2018-K47. *https://minorplanetcenter.net/mpec/K20/K20RG6.html*

Beniyama, J.; Baransky, A.; Khorolsky, A.; Solomakha, M.; Pettarin, E.; Panterotto, G.; Wiggins, P.; James, N.; Bolin, B.T.; Bhalerao, V.; Copperwheat, C.M.; Deshmukh, K.P.; Hsu, C.-Y.; Lin, Z.-Y.; Purdum, J. and 33 colleagues (2020). "2020 UQ6" *MPEC* 2020-U259. *https://minorplanetcenter.net/mpec/K20/K20UP9.html*

Buzzi, L.; Pettarin, E.; Hug, G.; Cromer, D.; Valentine, R.; James, N.; Bulger, J.; Chambers, K.; Lowe, T.; Schultz, A.; Willman, M.; Chastel, S.; Huber, M.; Ramanjooloo, Y.; Wainscoat, R. and 16 colleagues (2020). "2020 RA6" *MPEC* 2020-R166. *https://minorplanetcenter.net/mpec/K20/K20RG6.html*

Harris, A.W.; Young, J.W.; Scaltriti, F.; Zappala, V. (1984). "Lightcurves and phase relations of the asteroids 82 Alkmene and 444 Gyptis." *Icarus* **57**, 251-258.

Harris, A.W.; Young, J.W.; Bowell, E.; Martin, L.J.; Millis, R.L.; Poutanen, M.; Scaltriti, F.; Zappala, V.; Schober, H.J.; Debehogne, H.; Zeigler, K. (1989). "Photoelectric Observations of Asteroids 3, 24, 60, 261, and 863." *Icarus* **77**, 171-186.

Jahn, J.; Bulger, J.; Lowe, T.; Schultz, A.; Willman, M.; Chambers, K.; Chastel, S.; de Boer, T.; Denneau, L.; Fairlamb, J.; Flewelling, H.; Huber, M.; Lin, C.-C.; Magnier, E.; Ramanjooloo, Y. and 7 colleagues (2020). "2020 TD8" *MPEC* 2020-U97. *https://minorplanetcenter.net/mpec/K20/K20U97.html*

Number	Name	Integration times	Max intg. / Period	Min a/b	Points	Fields	Acquiring images for	Total Span	Run#	Run times (2020) mm/dd From-To
	2018 KF1	3.4-3.6	0.03	1.5	1498	29	2 h 47 m	3 h 15 m		
	2020 GF2	2,4.2-4.6	0.07	1.5	1417	24	2 h 31 m	3 h 14 m		
	2020 OH3	1,4	0.003	1.5	1076	13	2 h 00 m	2 h 33 m		
	2020 RA6	1,44$^{\Sigma}$	0.04	1.7	491	11	0 h 29 m	3 h 45 m		
					365	8			1	09/17 20:13-20:35
					126	3			2	09/17 23:35-23:58
	2020 RZ6	1,1.5	0.05	1.3	550	14	0 h 40 m	6 h 44 m		
					294	6			1	09/17 19:46-20:10
					93	3			2	09/18 00:03-00:15
					163	5			3	09/18 02:19-02:38
	2020 TP1	16	0.01	1.8	596	6	3 h 15 m	4 h 30 m		
					266	3			1	10/09 19:31-21:07
					330	3			2	10/09 22:17-10/10 00:01
	2020 TD8	2,3	0.10	1.4	582	10	1 h 02 m	3 h 44 m		
	2020 UQ6	10	0.06	1.5	440	6	1 h 55 m	2 h 40 m		
	2020 VZ6	8,12	0.03	1.5	333	4	1 h 12 m	1 h 15 m		
	2020 XX3	10,16	0.12	1.6	394	6	1 h 35 m	1 h 40 m		

Table I. Ancillary information, listing the integration times used (seconds), the fraction of the period represented by the longest integration time (see Pravec et al., 2000), the calculated minimum elongation of the asteroid (Kwiatkowski et al., 2010), the number of data points used in the analysis, the number of times the telescope was repositioned to different fields, the total elapsed time actively acquiring images, the time span of first to last image used in the analysis and run details where gaps in coverage are significant, including Run number and start-end date/times. Note: Σ = Longest elapsed integration time for stacked images (start of first to end of last exposure used).

Number	Name	yyyy mm/ dd	Phase	L_{PAB}	B_{PAB}	Period(h)	P.E.	Amp	A.E	Grp	H
	2018 KF1	2018 05/20-05/21	56.6,57.4	250	27	0.0317410	0.0000009	1.3	0.2	NEA	25.8
	2020 GF2	2020 04 11-04/12	25.0,30.1	205	14	0.0185620	0.0000005	0.75	0.15	NEA	26.0
	2020 OH3	2020 07/22-07/23	42.2,43.1	322	2	0.3923	0.0002	1.0	0.2	NEA	24.6
	2020 RA6	2020 09/17-09/17	71.1,93.9	12	38	0.3423	0.0001	2.1	0.2	NEA	26.0
	2020 RZ6	2020 09/17-09/18	86.2,103.0	41	20	0.0088557	0.0000001	1.2	0.3	NEA	26.6
	2020 TP1	2020 10/09-10/10	8.5,8.6	18	4	0.4167 NPA?	0.0004	0.8	0.2	NEA	26.8
	2020 TD8	2020 10/26-10/27	53.9,59.9	58	15	0.0082110	0.0000002	0.9	0.2	NEA	26.9
	2020 UQ6	2020 10/27-10/28	23.8,25.8	47	-4	0.045210	0.000002	0.74	0.09	NEA	22.6
	2020 VZ6	2020 12/01-12/01	33.2,33.1	54	-5	0.09804	0.00009	0.8	0.3	NEA	25.2
	2020 XX3	2020 12/17-12/17	31.7,32.3	69	1	0.038024	0.000009	1.0	0.2	NEA	28.5

Table II. Observing circumstances and results. The phase angle is given for the first and last date. If preceded by an asterisk, the phase angle reached an extrema during the period. L_{PAB} and B_{PAB} are the approximate phase angle bisector longitude/latitude at mid-date range (see Harris et al., 1984). Grp is the asteroid family/group (Warner et al., 2009), and H is the absolute magnitude at 1 au from Sun and Earth taken from the Small-Body Database Browser (JPL, 2020a). Note: NPA? = Possible Non-Principal Axis rotation.

JPL (2020a). Small-Body Database Browser *https://ssd.jpl.nasa.gov/sbdb.cgi*

JPL (2020b). Sentry: Earth Impact Monitoring Impact Risk Data *https://cneos.jpl.nasa.gov/sentry/*

Kwiatkowski, T.; Buckley, D.A.H.; O'Donoghue, D.; Crause, L.; Crawford, S.; Hashimoto, Y.; Kniazev, A.; Loaring, N.; Romero Colmenero, E.; Sefako, R.; Still, M.; Vaisanen, P. (2010). “Photometric survey of the very small near-Earth asteroids with the SALT telescope - I. Lightcurves and periods for 14 objects.” *Astron. Astrophys.* **509**, A94.

Melnikov, S.; Hoegner, C.; Stecklum, B.; Mikuz, B.; Jaeger, M.; Prosperi, E.; Prosperi, S.; Foglia, S.; Galli, G.; Buzzi, L.; Donati, S.; Biagini, F.; Simon, A.; Baransky, A.; Zoltowski, F.B. and 47 colleagues (2020a). “2020 GF2” *MPEC* 2020-G86. *https://minorplanetcenter.net/mpec/K20/K20G86.html*

Melnikov, S.; Stecklum, B.; Buzzi, L.; Gilmore, A.C.; Kilmartin, P.M.; Bulger, J.; Chambers, K.; Lowe, T.; Schultz, A.; Willman, M.; Chastel, S.; Huber, M.; Ramanjooloo, Y.; Wainscoat, R.; Weryk, R. and 21 colleagues (2020b). “2020 OH3” *MPEC* 2020-O92. *https://minorplanetcenter.net/mpec/K20/K20O92.html*

MPC (2020) Minor Planet Center NEO Confirmation Page *https://www.minorplanetcenter.net/iau/NEO/toconfirm_tabular.html*

Panterotto, G.; Pettarin, E.; Bulger, J.; Lowe, T.; Schultz, A.; Willman, M.; Chambers, K.; Chastel, S.; de Boer, T.; Denneau, L.; Fairlamb, J.; Flewelling, H.; Huber, M.; Lin, C.-C.; Magnier, E. and 23 colleagues (2020). “2020 VZ6” *MPEC* 2020-W192. *https://minorplanetcenter.net/mpec/K20/K20WJ2.html*

Pettarin, E.; James, N.; Bolin, B.T.; Bhalerao, V.; Copperwheat, C.M.; Deshmukh, K.P.; Hsu, C.-Y.; Lin, Z.-Y.; Purdum, J.; Sharma, K.; Zhai, C.; Z.T.F. Collaboration; Duev, D.A.; Lin, H.-W.; Masci F.J. and 16 colleagues (2020). “2020 TP1” *MPEC* 2020-T55. *https://minorplanetcenter.net/mpec/K20/K20T55.html*

Pravec, P.; Hergenrother, C.; Whiteley, R.; Sarounova, L.; Kusnirak, P.; Wolf, M. (2000). “Fast Rotating Asteroids 1999 TY2, 1999 SF10, and 1998 WB2” *Icarus* **147**, 477-486.

Pravec, P.; Harris, A.W.; Scheirich, P.; Kušnirák, P.; Šarounová, L.; Hergenrother, C.W.; Mottola, S.; Hicks, M.D.; Masi, G.; Krugly, Yu.N.; Shevchenko, V.G.; Nolan, M.C.; Howell, E.S.; Kaasalainen, M.; Galád, A. and 5 colleagues (2005). “Tumbling Asteroids.” *Icarus* **173**, 108-131.

Raab, H. (2018). Astrometrica software, version 4.12.0.448. *http://www.astrometrica.at/*

Read, M.T.; Bulger, J.; Lowe, T.; Schultz, A.; Willman, M.; Chambers, K.; Chastel, S.; de Boer, T.; Denneau, L.; Fairlamb, J.; Flewelling, H.; Huber, M.; Lin, C.-C.; Magnier, E.; Ramanjooloo, Y. and 31 colleagues (2020). “2020 XX3” MPEC 2020-X132. *https://minorplanetcenter.net/mpec/K20/K20XD2.html*

Tichy, M.; Ticha, J.; Dupouy, P.; Holmes, R.; Foglia, S.; Buzzi, L.; Linder, T.; Hug, G.; Losse, F.; Birtwhistle, P.; Adamovsky, M.; Korlevic, K.; Lyon, I.; Denneau, L.; Tonry, J. and 13 colleagues (2020). “2020 RZ6” MPEC 2020-S16. *https://minorplanetcenter.net/mpec/K20/K20S16.html*

Warner, B.D.; Harris, A.W.; Pravec, P. (2009). “The Asteroid Lightcurve Database.” *Icarus* **202**, 134-146. Updated 2020 Oct. *http://www.MinorPlanet.info/lightcurvedatabase.html*

Warner, B.D. (2020). MPO Software, *MPO Canopus* v10.8.2.8. Bdw Publishing, Eaton, CO. *http://minorplanetobserver.com*

Wells, G.; Bamberger, D. (2020). “2020 UQ6”. *https://twitter.com/NBObservatories/status/1322554380923666434*